

Article

Structural & Tectonic Evolution of the Porgera Gold Mine; Highlands of Papua New Guinea

Kevin C. Hill¹, Gareth T. Cooper², Agnes Pokondepa³, Peter Essy³, Thiwaporn Phonsit¹ and Mark Haydon³

1. School of Geography, Earth and Atmospheric Sciences, University of Melbourne, Parkville, Victoria, Australia
 2. Enigma Energy Services in Hobart, Tasmania, Australia
 3. Porgera Joint Venture, working with Barrick Niugini Ltd
- * Correspondence: Corresponding Author: Kevin Hill, kevin.hill@unimelb.edu.au

Abstract: The acquisition of regional, 1 metre resolution LIDAR in the PNG Highlands combined with 3D modelling in MoveTM has revolutionized our understanding of the evolution of the Porgera gold mine and areas of new potential. The new 3D model demonstrates active pull-apart basins along a regional transfer during ongoing fold and thrust deformation. When overlain on regional aeromagnetic data, new potential is revealed.

The Porgera gold mine is one of the richest in the world and lies in a wide valley at an elevation of 2800m surrounded by mountains up to 4000m high in the middle of the PNG Highlands. It lies along a major lineament, the Porgera Transfer Zone (PTZ), cutting across the orogen that is associated with a 50 km offset of the ophiolite belt. To the NW of the mine there is an extensive belt of low- to high-grade metasediments that formed in deep water during Jurassic rifting, but were metamorphosed during Eocene subduction to the north. Subduction ceased due to accretion of the Sepik Terrane which caused inversion and mild erosion of the Porgera area. The Late Oligocene onset of wrenching in the Mobile Belt to the north placed that area into extension, emplacing metamorphic core complexes, and led to regional subsidence in the Early Miocene. Collision of the margin with the Melanesian Arc in the Middle Miocene caused Late Miocene to Pliocene orogenesis creating the broad mountain belt that we see today, that is still active, as shown by the 2018 Mw 7.5 earthquake.

Regional mapping of the area using high resolution LIDAR in association with limited field mapping, analysis of gravity and magnetics data and drilling of 300-500m deep core-holes has allowed development of a detailed 3D structural model. The Porgera valley is constrained laterally by the Eastern Boundary and Western Boundary dextral strike-slip faults that lie along the PTZ cutting across the orogeny. However, whilst the position and nature of the faults is clear, due to bending, fracturing and offset of major synclines and anticlines, the faults do not crop-out as significant through-going features. Rather, the dextral offset of basement is soft-linked to the Tertiary limestones at surface due to intervening thick, ductile Cretaceous shales. Fold and thrust structures are ubiquitous in the Tertiary limestones, but the youngest structural features are large extensional faults, particularly around the Porgera valley.

The intrusive underlying the Porgera ore-body was emplaced at 6.0±0.3 Ma, the time of maximum compression during orogenesis. At this time the Eastern Boundary fault and Western Boundary fault were both active allowing a pull-apart basin to form locally along the PTZ at the south-eastern boundary of the Jurassic metasediments. This enabled emplacement of the intrusive. The gold-bearing fluids from the intrusive and metasediments were brought up through the Mesozoic muds to the contact with the Paleogene carbonates where the Porgera ore body was emplaced.

Keywords: Fold belt; Metasediments; Ore-body; Orogenesis; Pull-apart basin

Introduction

The island of New Guinea lies along the northern margin of the Indo-Australian plate where it is undergoing oblique convergence with the Pacific Plate (Figure 1 inset). Southern New Guinea comprises relatively undeformed Australian crust that is bowed down in the west to form a foreland basin in front of the Fold Belt mountains (Hill & Hall 2003). The Fold Belt comprises a broad zone of folded and thrust Jurassic-Pliocene sediments that were deposited along the northern Australian margin. It is underlain by extensional faults formed during Jurassic rifting some of which were reactivated during the Late Miocene to Pliocene compression (Figure 1). The Fold Belt is bound to the north by a Mobile Belt (shown very schematically on Figure 1) comprising distal sediments, ophiolites, igneous and metamorphic rocks. It is bound to the north by the Paleogene Melanesian arc that collided in the Middle Miocene causing orogenesis of the margin.

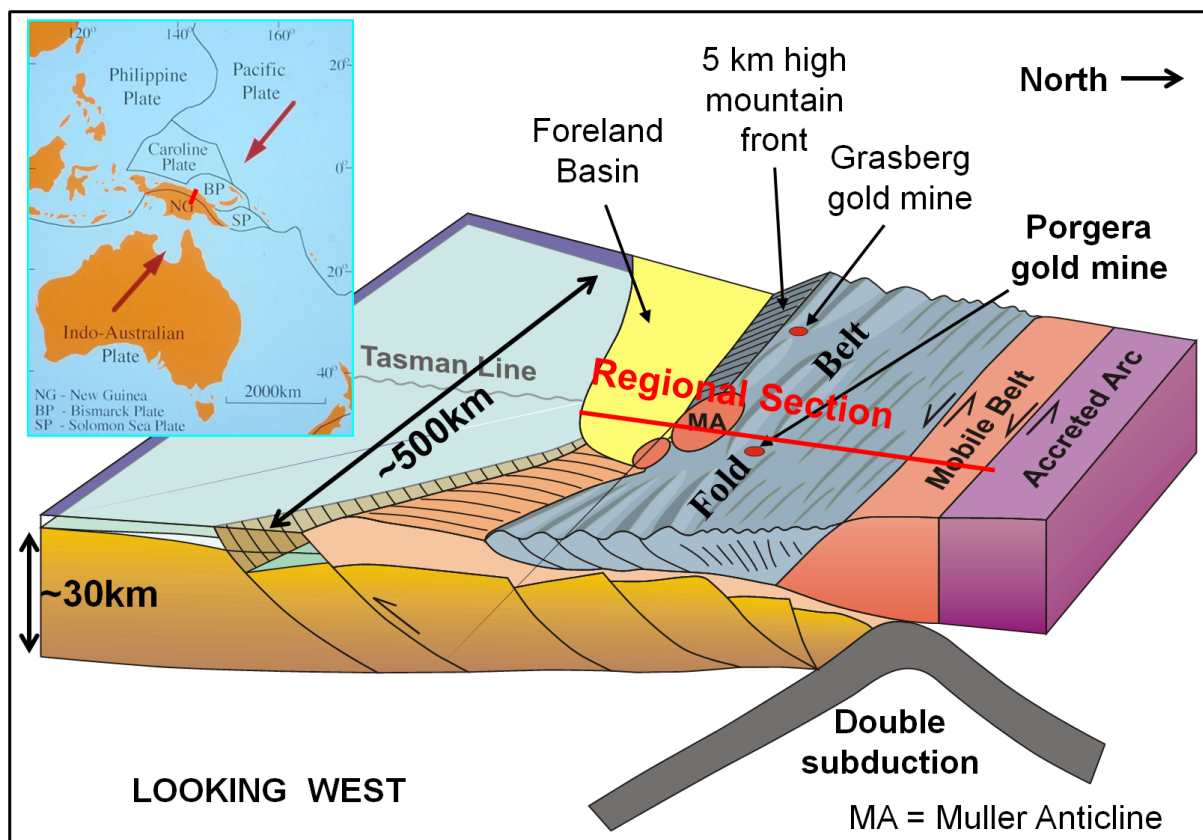


Figure 1. Plate tectonic setting of New Guinea (inset) and a block diagram illustrating the structure of the margin, after Hill & Hall (2003, their Figure 13). The location of the regional section in Figure 4 is shown on both the block diagram and the inset by a red line.

Hill & Hall (2003) considered that the margin underwent extension and rifting in the Early to Middle Jurassic leading to Late Jurassic breakup and passive margin subsidence in the Early Cretaceous. Renewed Late Cretaceous rifting led to a second period of breakup in the latest Cretaceous leading to drifting away of the Sepik Terrane (Zahirovic et al 2014). The Eocene onset of rapid northward movement of the Australian Plate caused the Sepik terrane to dock with northern PNG in the Oligocene (Crowhurst et al 1996; see location on Figure 2) inverting parts of the PNG margin (Mahoney et al 2019) prior to Early Miocene extension and subsidence. The ongoing rapid northward movement of the Australian Plate generated subduction to the north remote from New Guinea creating the Melanesian island arc that collided obliquely with PNG in the Middle Miocene causing Late Miocene to Present orogenesis and compression.

Along the PNG margin in the Middle Miocene there was substantial volcanism associated with emplacement of the Maramuni Arc above the southward-subducting slab

shown in Figure 1 (Hill & Hall 2003). However, this volcanism declined significantly with the onset of compression in the Late Miocene. Traversing the Fold Belt there are some lines of volcanoes, such as the Bosavi lineament, and Pliocene volcanic stocks that get younger to the south (Davies 1991). Corbett (1994) and Hill et al (2002) suggested that these lines were controlled by an underlying NNE trending fabric in basement within which there were local reactivated NNE-trending shear zones.

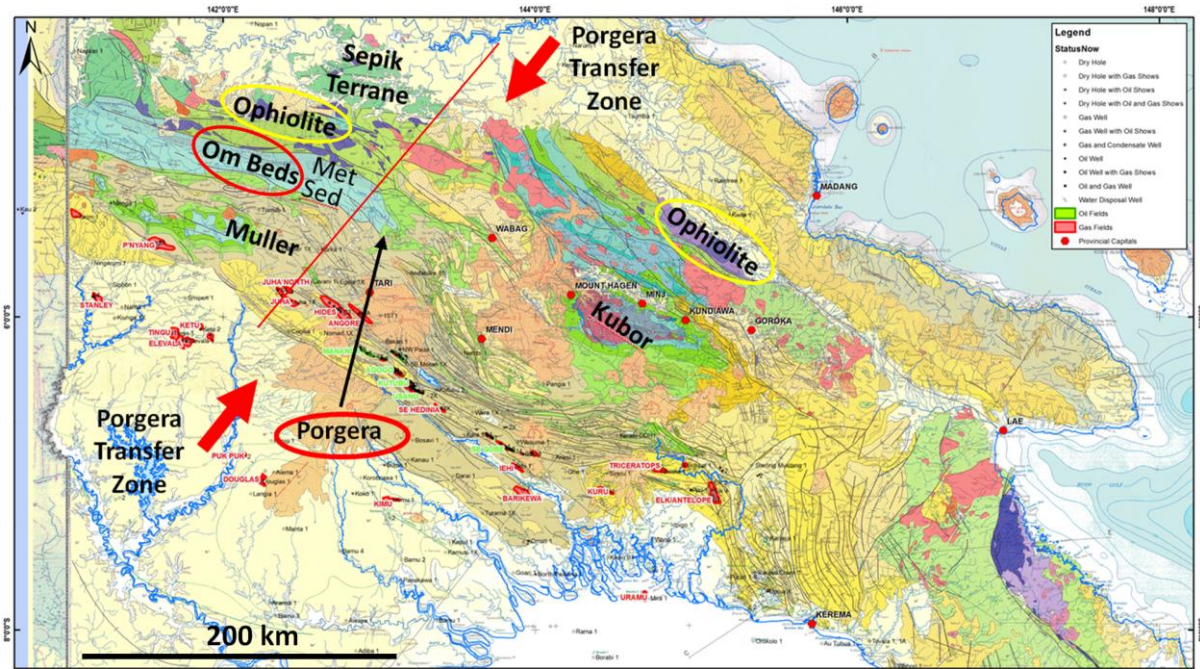


Figure 2. Geological map of western PNG showing the location of the Porgera Transfer Zone and how it accommodates offset of the ophiolites (purple) by over 50 km. The red line shows the location of the cross-section in Figure 4. Note the location of the Om Beds that formerly filled the Om Basin.

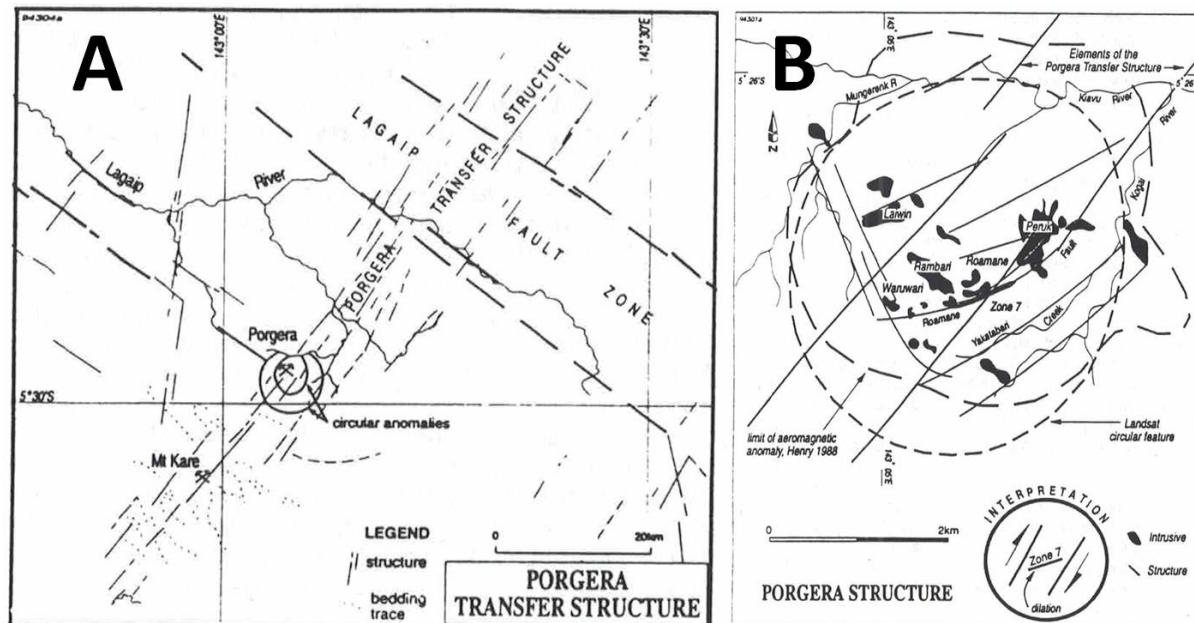


Figure 3. A) The Porgera Transfer Structure and the anomalies around the mine and B) a close up of the mine intrusives with a model for dilation with dextral movement across the Transfer, both from Corbett (1994).

The Porgera Intrusive Complex (PIC) was emplaced at 6.0 ± 0.3 Ma (Richards & McDougall 1990) along the Porgera Transfer Zone (Corbett 1994) in the northern portion

of the PNG Fold Belt (Figures 2 and 3). The mesothermal/epithermal gold mineralisation occurs in structurally controlled veins and disseminations which overprint and cross-cut a suite of shallow-level, comagmatic, mafic alkaline stocks and dykes (Richards & McDougall 1990). These are hosted in friable black mudstones of the Chim Formation of uppermost Cretaceous age (Gunson et al 2000).

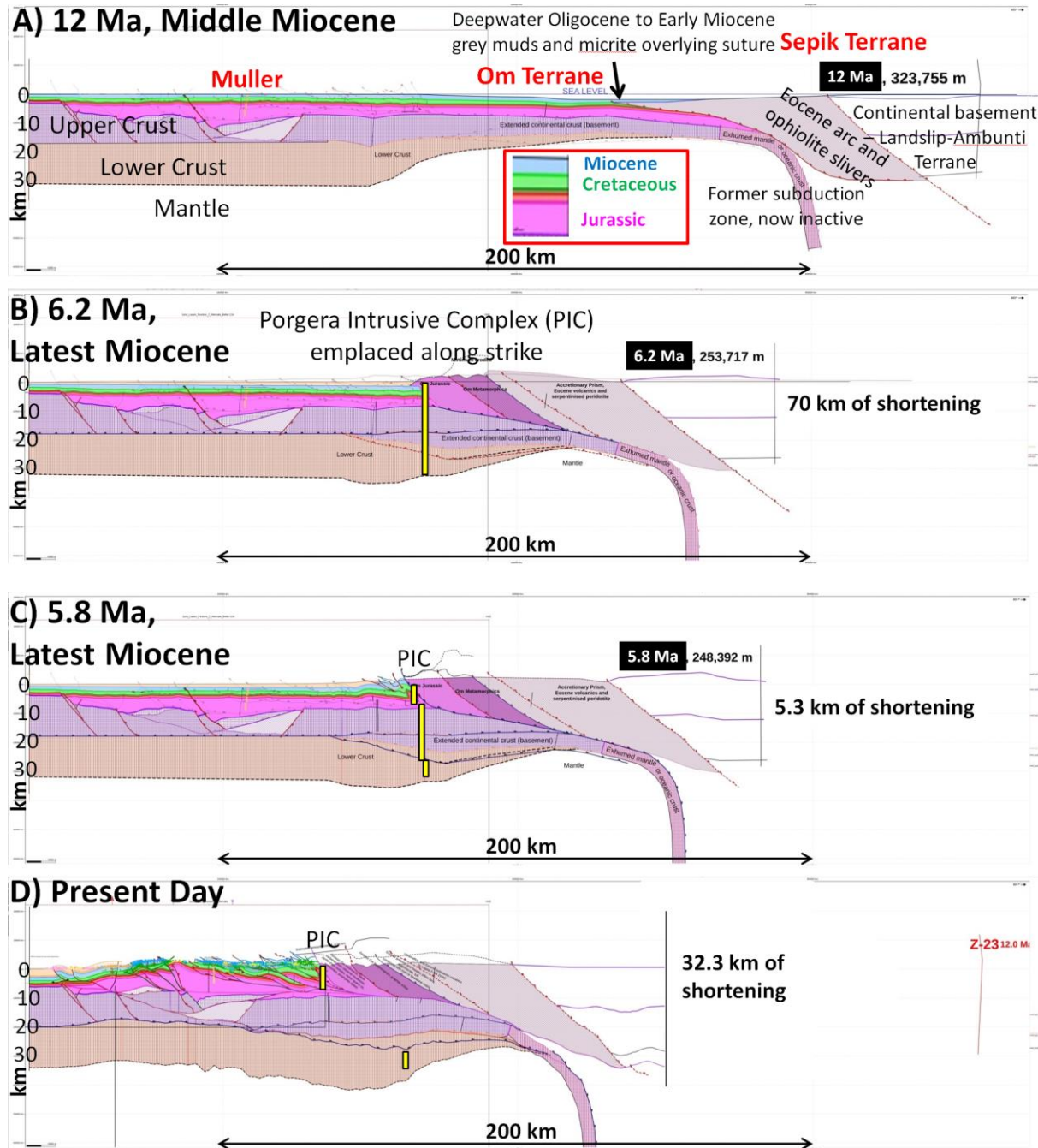


Figure 4. Structural evolution of a regional cross-section near the Porgera mine. See Figures 1 and 2 for section location and text for details. After Hill et al (2020).

Structural setting

The Porgera Transfer Zone (PTZ) is readily apparent on a geological map (Figure 2). It coincides with the eastern plunging nose of the basement-cored Muller Anticline and the plunging nose of the Jurassic syn-rift Om beds (Figure 2). It aligns with the eastern edge of the Sepik Terrane and with a 50 km sinistral offset of the leading edge of the ophiolites (see Hill et al 2002 for more details). A regional cross section has been constructed

from the Juha Anticline at the leading edge of the Fold Belt to the Sepik Terrane and has been balanced and restored (Hill et al 2020). The section is shown in Figure 4 and its position is shown on Figures 1 and 2, 25 km west of the PTZ and parallel to it.

Section A shows the pre-compression geometry of the margin at ~12 Ma (Figure 4). The section shows large extensional, rift faults in the Jurassic beneath the Muller Anticline and these probably continue further north but are unproven. The upper and lower crust are interpreted to thin to the north as part of the Jurassic and Cretaceous rifting and break-up processes. The Cretaceous sequence is inferred to be relatively constant in thickness, but there may be extensional faults and growth sequences in the northern region above the thinned crust. The Miocene sequence is also relatively constant in thickness, consistent with regional subsidence of the margin, but it thins to the north where it passes from reefal carbonates into deep-water mudstones. Importantly, some of these muds and micrites are interpreted to lie across the suture between the Ophiolites/Eocene volcanics of the Sepik Terrane and the PNG margin sediments. An inactive subduction zone is shown beneath the Sepik Terrane which is a remnant from when it docked with the PNG margin in the Oligocene. Please note that the crustal thickness is approximate as it is only shown schematically.

Around 12 Ma the Melanesian Arc collided with the northern edge of the Sepik Terrane and shunted it onto the PNG margin (Section B, Figure 4). There was relatively little shortening within the Sepik Terrane itself, but from 12 Ma to 6.2 Ma there was ~70 km shortening of the PNG margin. This shortening was mainly within the Om Beds, the northern portion of which was substantially uplifted and eroded exposing medium to high-grade metamorphic rocks at the surface. However, there was a similar amount of shortening and thickening of the crust beneath the Om Beds, here shown schematically as a triangle zone in basement. Please note that the PIC was emplaced along strike at ~6 Ma during maximum compression which is problematic (see later). It is here shown schematically as an intrusive from the mantle.

From 6.2 Ma to 5.8 Ma, during emplacement of the PIC, the section was shortened by a further 5.3 km as shown on Section C. The thrusting would have dismembered the igneous pipe that fed the PIC, shown schematically on Section C. From 5.8 Ma to the Present there was a further 32.3 km of shortening within the PNG Fold Belt as shown on section D and in more detail in Hill et al (2020). The igneous pipe that fed the PIC was probably further dismembered and is not shown in detail here.

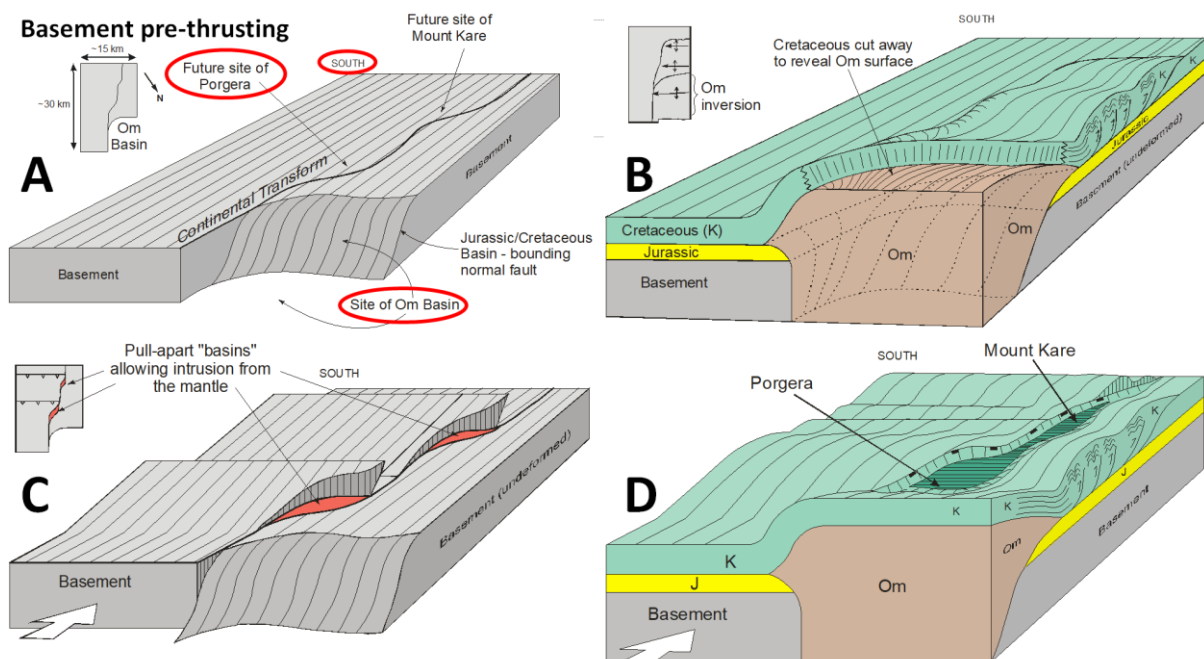


Figure 5. A structural model for the evolution of the Porgera complex, looking south at the Porgera Transfer Zone from the northern side of Figure 2 (Hill et al 2004; courtesy of Porgera JV). See text for details.

A tectonic model for emplacement of the Porgera Intrusive Complex

Figure 4 shows that the PIC was emplaced during a time of maximum compression, so a model is needed to provide dilation so that the magma can ascend through the thickening crust. Hill (2004) suggested that this was caused by differential movement across the PTZ, an old basement fault zone that was reactivated (Figure 5). Figure 5A shows a 3D view and map of the continental crust (basement) looking to the south across the PTZ. During Jurassic rifting the margin had a step-shape such that there was an embayment with oceanic crust in the Om region adjacent to normal thickness crust to the east, which was a continental promontory. This is similar to the Jurassic oceanic crust of the Argo Abyssal Plain next to the continental promontory of the Exmouth Plateau on today's NW Shelf of Australia. The Jurassic, Cretaceous and Paleogene/Miocene sediments were deposited across the margin, with substantial thickening of the Om Beds into the embayment. For simplicity, the Paleogene/Miocene sediments are not shown on Figures 5B and 5D.

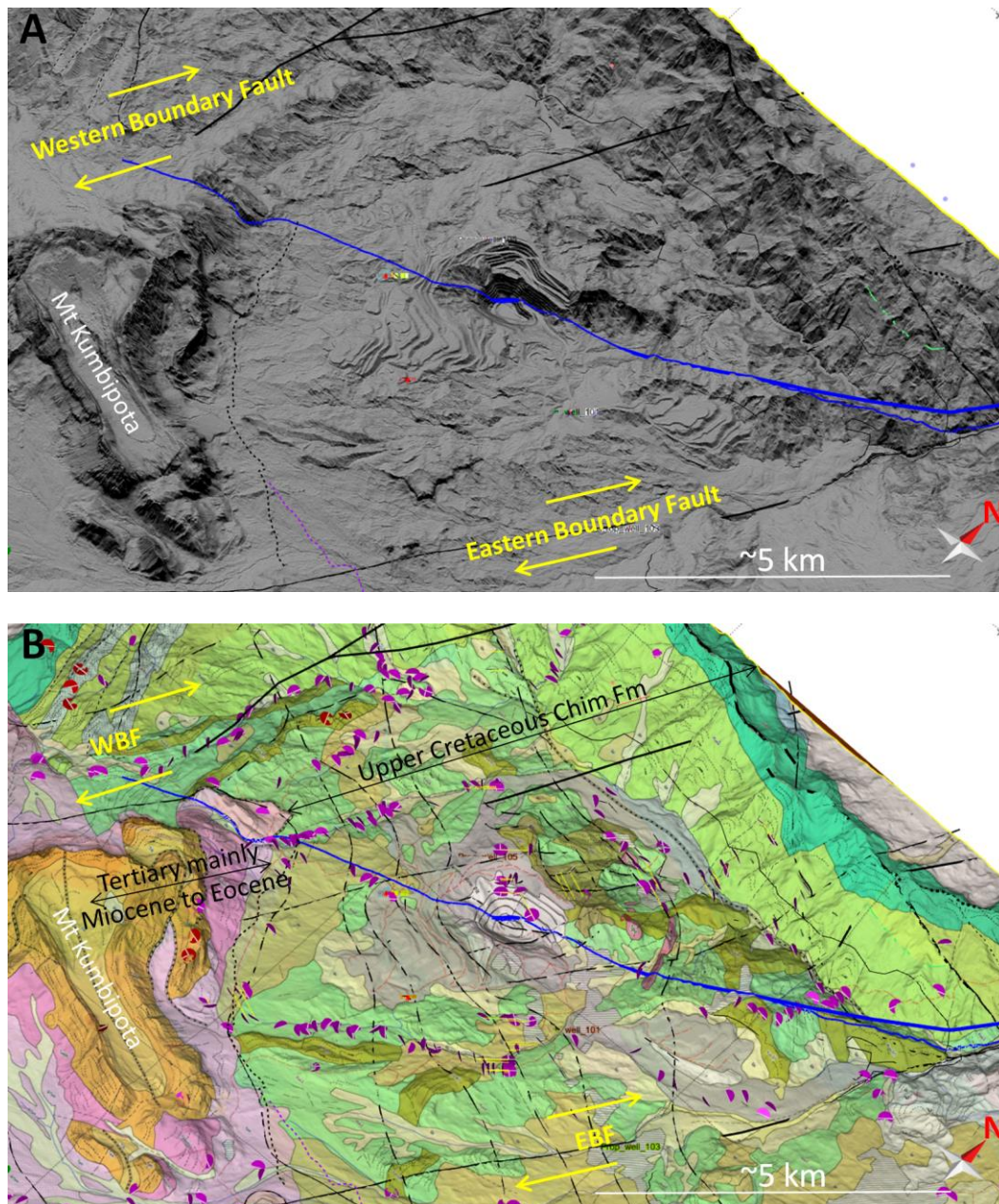
At the onset of compression in the Middle Miocene it is inferred that the Om beds were inverted causing thin-skinned compression of the Cretaceous and Tertiary sequence to the south as shown on Figure 5B. Probably at the same time, there was substantial shortening of the continental promontory to the east of the PTZ as shown on Figure 5C. Small offsets across the PTZ led to the local development of strike-slip pull-apart basins along the PTZ allowing intrusive rocks from the mantle to ascend. Figure 5D shows the combined effects of B and C. At the same time as folding and thrusting occurred both to the east and west of the PTZ, there was extensional collapse into the local pull-apart basins along it. The rising magma encountered shattered Mesozoic and Tertiary sediments within the collapse grabens and gold was precipitated in the upper most Cretaceous shales at the contact with the Tertiary marls and carbonates.



Figure 6. An aerial view of the Porgera gold mine, showing the steep jungle-covered terrain and the high elevation.

Testing the tectonic model – LIDAR and cross-sections

Within the Fold Belt, the Porgera gold mine lies in a valley at an elevation of ~2500m surrounded by mountains at an elevation of 3500m to almost 4000m (Figure 6). The terrain is mountainous with only one road and is heavily vegetated by either tropical forest or impenetrable, 2-3 metre tall Kunai grass. Outcrop is generally scarce except in the cliffs and some creeks. Around the mine there are many shallow boreholes providing samples and stratigraphic sections (Gunson et al 1997) but elsewhere relatively few outcrops have been recorded, mainly by Thornton et al (1996) and Davies (1983). To improve mapping of the area, the Porgera JV acquired high resolution LIDAR data and spectral imaging in a strip continuing for 25 km to the south of the mine (Figure 7). The resolution on the LIDAR is to less than one metre and the datasets are vast.



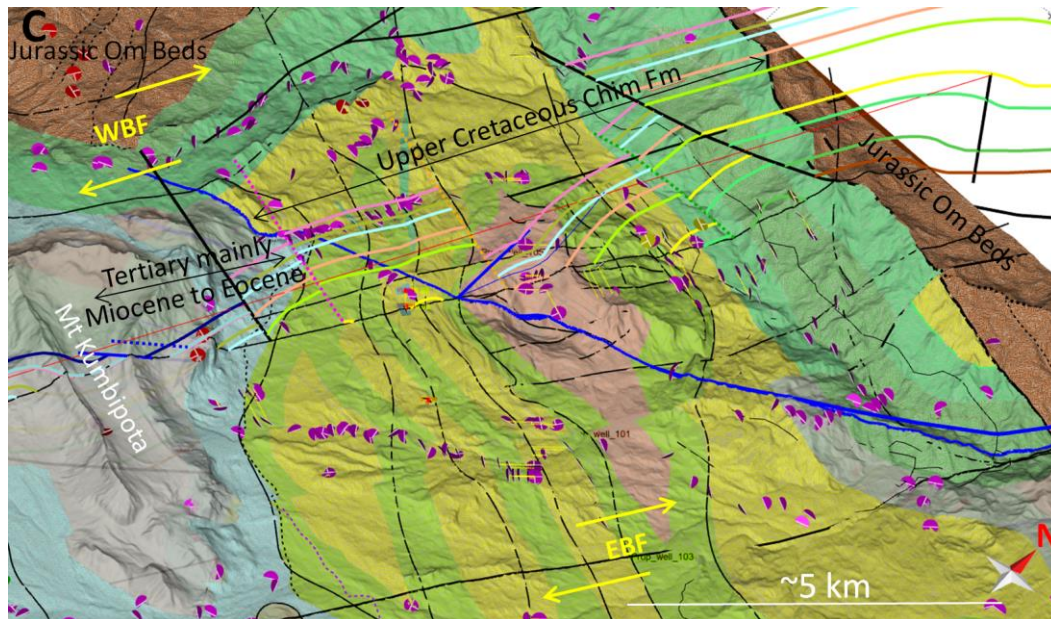


Figure 7. A) Oblique view of Bare Earth Lidar with sun shading in the area of the Porgera Mine, showing the location of the Eastern Boundary Fault (EBF) and Western Boundary Fault (WBF) and an interpretation of the oblique Roamane Fault in blue, cutting across the pit. B) The same Lidar as A with an air photo interpretation of geology displayed after Nash & Associates (2011) and dip data mainly from Gunson (2000) in purple. C) The same Lidar as A with geology displayed from this project after Gunson (2000), and showing the location of one of >100 sections constructed across the area in order to build the 3D model.

The data were entered into Move™ where the detailed topography could be overlain by geology maps (Figure 7) or the different spectral grids revealing different types of vegetation and bare rock. By sectioning the surface in the regional dip direction a good estimate of dip could be made in most areas, such as in the Kumbipota Syncline Figure 7A. Using the few surface data points and micro-palaeontological age dates a rough Tertiary and Upper Cretaceous stratigraphy was constructed, guided by the sections from Gunson et al (1997). This allowed the construction of >100 closely-spaced dip and strike sections across the area including the balanced and restored cross-section shown in Figure 8. The section presented (Figure 8D) was constructed by using dips and landforms that were correlated on the LIDAR and is increasingly speculative at depth, in particular the Jurassic section which is schematic.

A key feature of the section is the two normal faults, one through the mine and the other on the NE flank of Mount Kumbipota (Figure 8D). The latter is a SE continuation of a fault bounding the southern edge of the Jurassic Om Beds (Figure 2) and may be the basin-bounding fault suggested in Figure 5A. The fault through the mine is a representation of the Roamane Fault (blue line on Figure 7) an oblique extensional fault with 1-2 km of extensional offset that hosts most of the gold mineralisation. The remaining faults are listric thrust faults interpreted to detach within the Jurassic section. The section is presented to show the evolution of the structure but was balanced and restored in reverse order using the fault-parallel-flow and simple-shear algorithms in Move™. First, the normal faults were restored as well as two small backthrusts in the SW of the section (Figure 8C). Then the thrust faults were restored (Figure 8B) and finally the section was unfolded using the fault-bend-fold algorithm (Figure 8A). The final restored section contains minor kinks and anomalies from the restoration and could be improved, but it illustrates the evolution.

On Figure 8, section A represents the configuration of the margin in Miocene times pre-deformation. It is unclear if the Miocene Mala Limestone continued to the north, perhaps in a shaley facies, as no Miocene rocks are preserved. The section records growth to the NE in the Paleocene, Cretaceous and Jurassic across the Kumbipota normal fault

suggesting that this was a long-lived basin-bounding fault. With the onset of compression in the Late Miocene, the section was folded perhaps involving inversion of the basin bounding faults at depth as suggested on Figure 5B (Figure 8B). The section was then cut by thrust-faults with the underlying basin-bounding fault probably acting as a barrier, causing considerable compression and uplift to the north (Figure 8C). Finally, there was right-lateral movement across the Porgera Transfer opening pull-apart basins as shown in Figure 5C, with extensional faulting along the Kumbipota and Roamane Faults (Figure 8D) allowing emplacement of the Porgera Intrusive Complex (not shown). It is likely that stages B, C and D may have overlapped substantially, but they are here shown sequentially for simplicity.

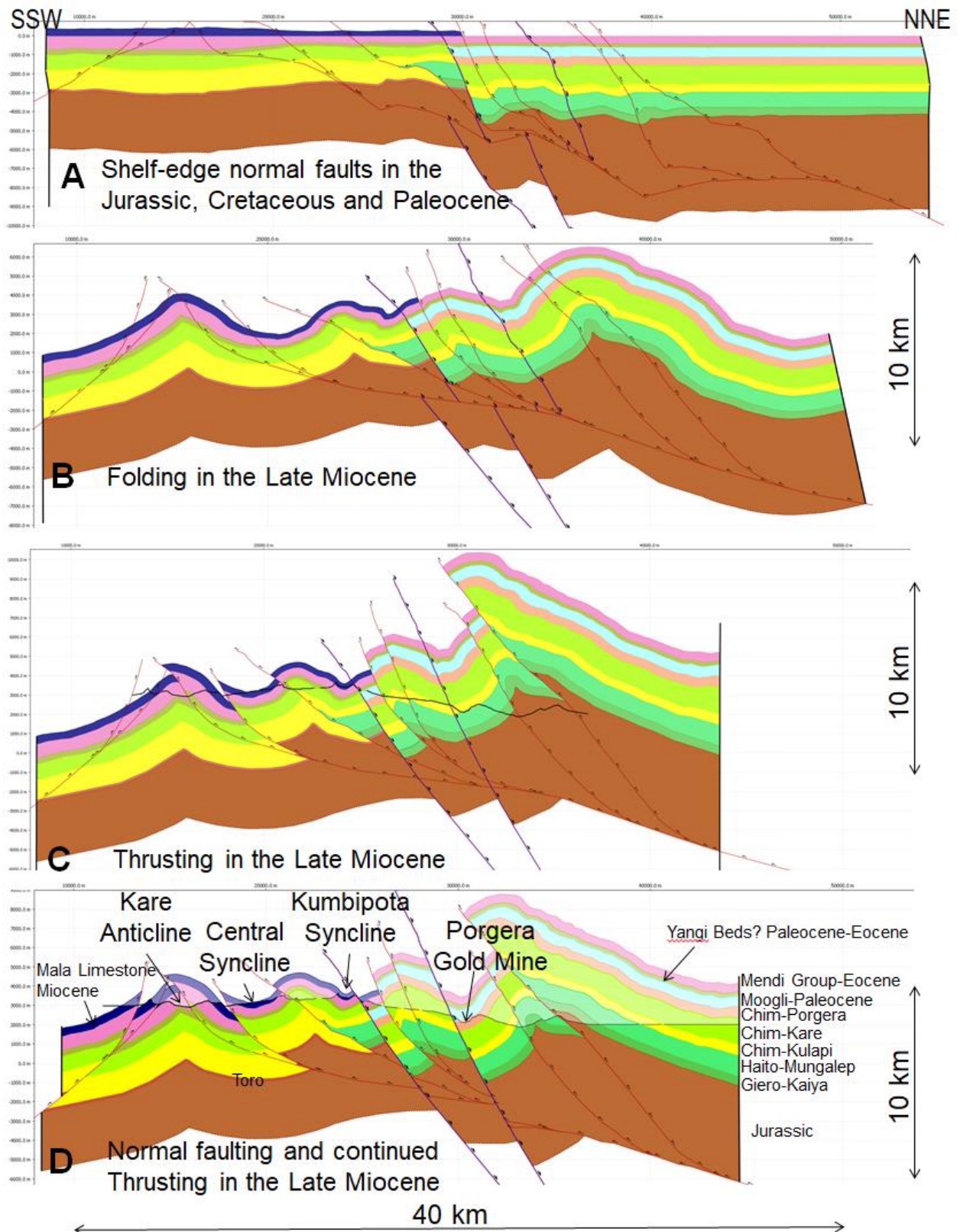


Figure 8. A balanced and restored cross-section through the Porgera gold mine. The section location is shown on Figures 7C and Figure 11. See text for details.

Examining the LIDAR surface on Figure 7A, it can be seen that the Porgera mine is in a relatively low-lying area bound to the east by the Eastern Boundary Fault (EBF) and to the west by the Western Boundary Fault (WBF). The blue line cutting across the image

is the previously interpreted Roamane Fault inferred by Richard & McDougall (1990) and others to be the main zone of mineralization in the mine

One goal of the study was to examine these areas to see if there was evidence of extensional collapse as predicted in the tectonic model shown in Figure 5. Figure 9 is looking west at the LIDAR data along the north flank of the Mount Kumbipota syncline. Around the Mount many limestone blocks can be seen that appear to have slumped down, as shown by the yellow arrows. These are interpreted to be normal faults that were active during or just after the time of compressional deformation. It is possible to infer more normal faults in the Cretaceous shales in the valleys, but they are less convincing. However, the age-dating from boreholes is consistent with some large normal faults around the mine.

Figure 10 is looking towards the SSW along the Eastern Boundary Fault marked by the valley with a gravel road. The EBF is interpreted to be a dextral strike-slip fault which was consistent with our observations that the anticline and syncline structures were not continuous across the fault. On both sides of the EBF, large normal faults are interpreted within the carbonates such that they slump down towards the EBF as in a rift valley or graben (see yellow arrows on Figure 10). This suggests that the EBF was a strongly transtensional fault with extensional faulting along it as it moved. The observed normal faults around the mine and along the EBF are both consistent with the tectonic model proposed in Figure 5 and the section in Figure 8.

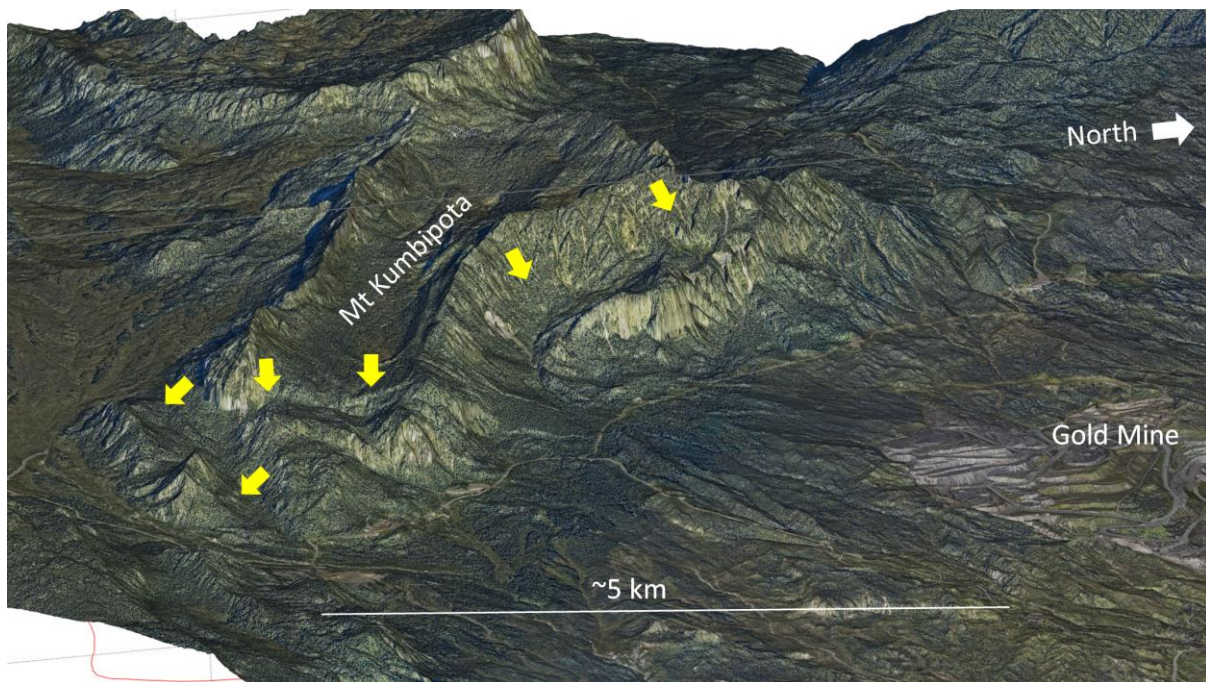


Figure 9. LIDAR data of the area south of the mine showing interpreted normal faults cutting the synclinal limestone outcrops in Mount Kumbipota. No vertical exaggeration.

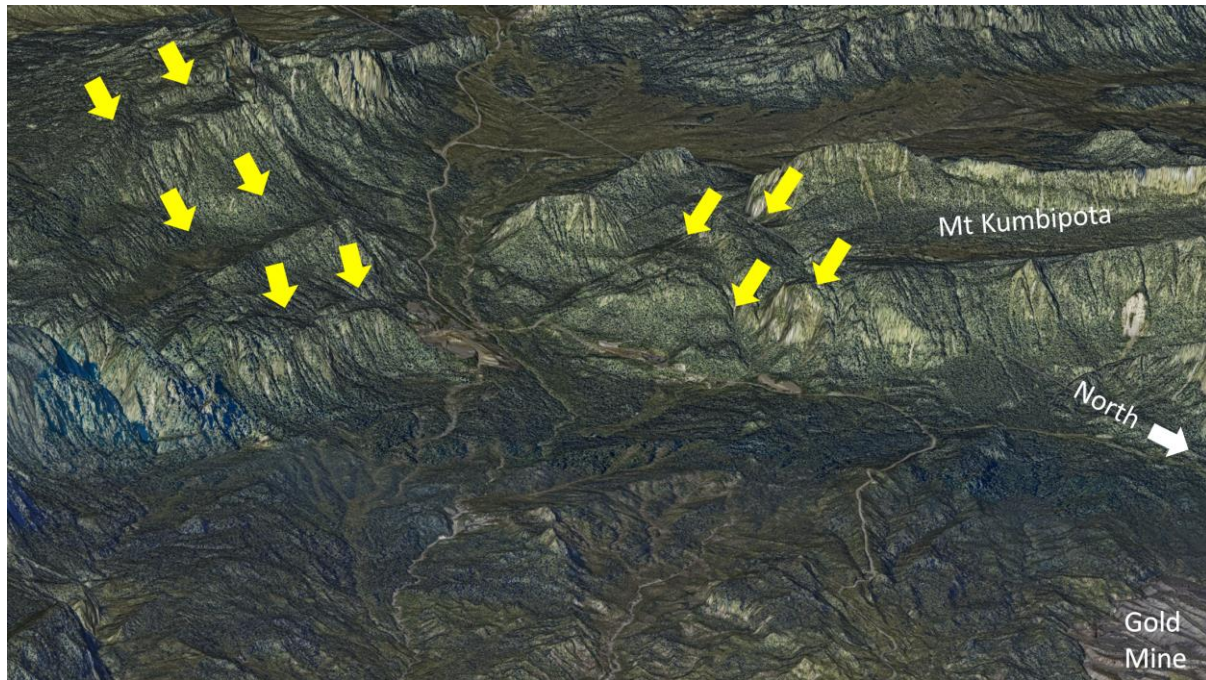


Figure 10. LIDAR data of the eastern end of Mount Kumbipota showing interpreted normal faults cutting the limestone cliffs. No vertical exaggeration.

3 D Model

Using the LIDAR data, the field data and micro-palaeontological dating and our inferred stratigraphic section, a 3D structural model of the area was constructed by tying the >100 cross-sections, as shown in Figures 11 and 12. In Figure 12 the faults are shown in red except the EBF shown in green. The model shows all the horizons reconstructed including those eroded above the surface to try to give an understanding of the geology. The pink horizon is interpreted to be the top of the Eocene limestone and is present across the whole model. The yellow and green horizons correspond to members of the Upper Cretaceous Chim Formation.

One standout feature is that the NW corner of the model, above the outcropping Jurassic Om Beds, has been uplifted around 4-5 km and eroded, here interpreted to have occurred along the 'Main Inversion Fault' (Figure 12) that continues to the NE of Mount Kumbipota (Figure 8). The km-scale uplift is supported by new palynological and thermal data (T_{max}/R_o) acquired as part of this study. To the south of the inversion fault, there are numerous low-angle thrust repeats creating anticlines and elevated synclines such as the Mount Kare anticline and Mount Kumbipota syncline. At the western end of the Mount Kumbipota syncline is the Western Boundary Fault (WBF, Figures 11 & 12) across which the top Eocene horizon is dropped down significantly on several large normal faults into the mine area. On Figure 12 the WBF is not shaded in order to allow the bed offset to be seen. At the eastern end of the Mount Kumbipota syncline there is an array of small normal faults in red, brown and green on Figure 12 that represent those observed in Figure 10, dropping down into a graben. It was observed that the EBF does not cut the Kare Anticline to the south, such that either displacement dies out to the south or it is transferred to the WBF on splays as can be seen in the complex fault array between Mount Kumbipota and Mount Kare on Figures 11 and 12. Figure 11 shows the 3D model truncated at the ground surface to make a geological map on which the EBF can be seen terminating against the northern flank of the Mount Kare Anticline.

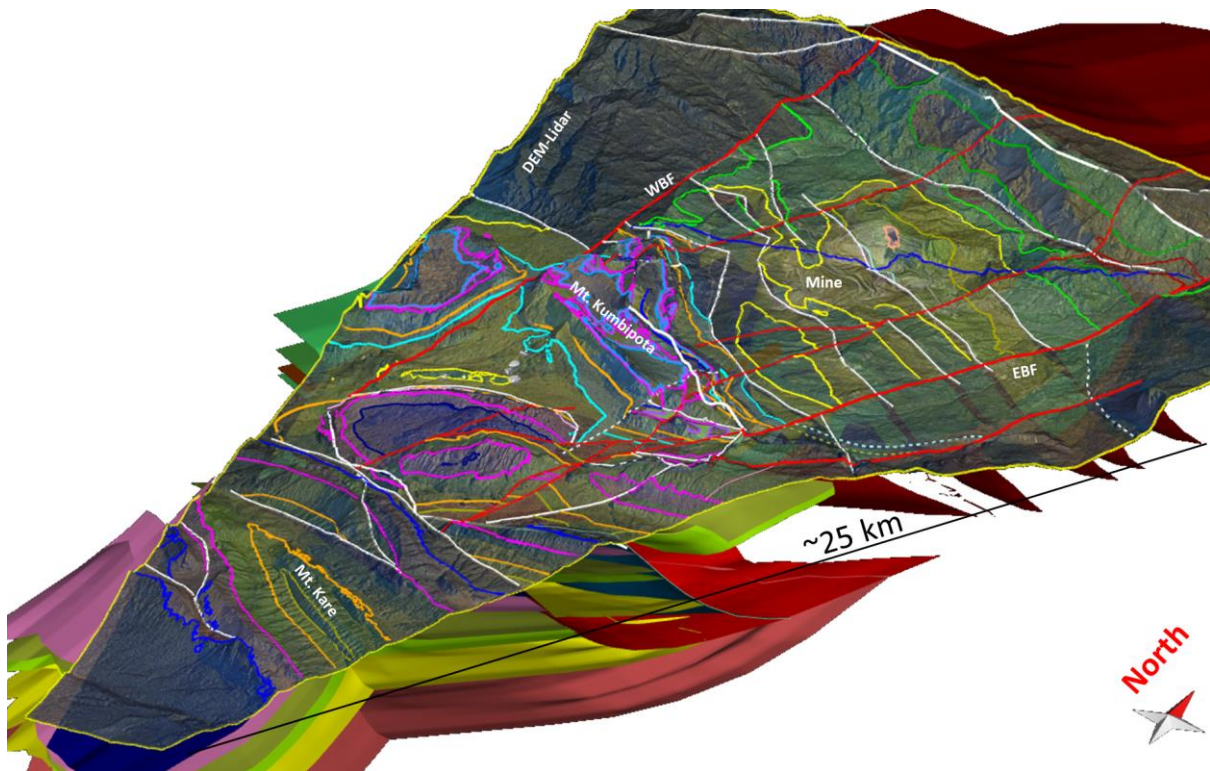


Figure 11. The 3D model constructed from ~100 cross-sections that were made using the LIDAR data. The LIDAR DEM is shown as well as surfaces below it. Faults are red. Horizons are coloured according to stratigraphy shown in Figure 8. EBF=Eastern Boundary Fault; WBF=Western Boundary Fault.

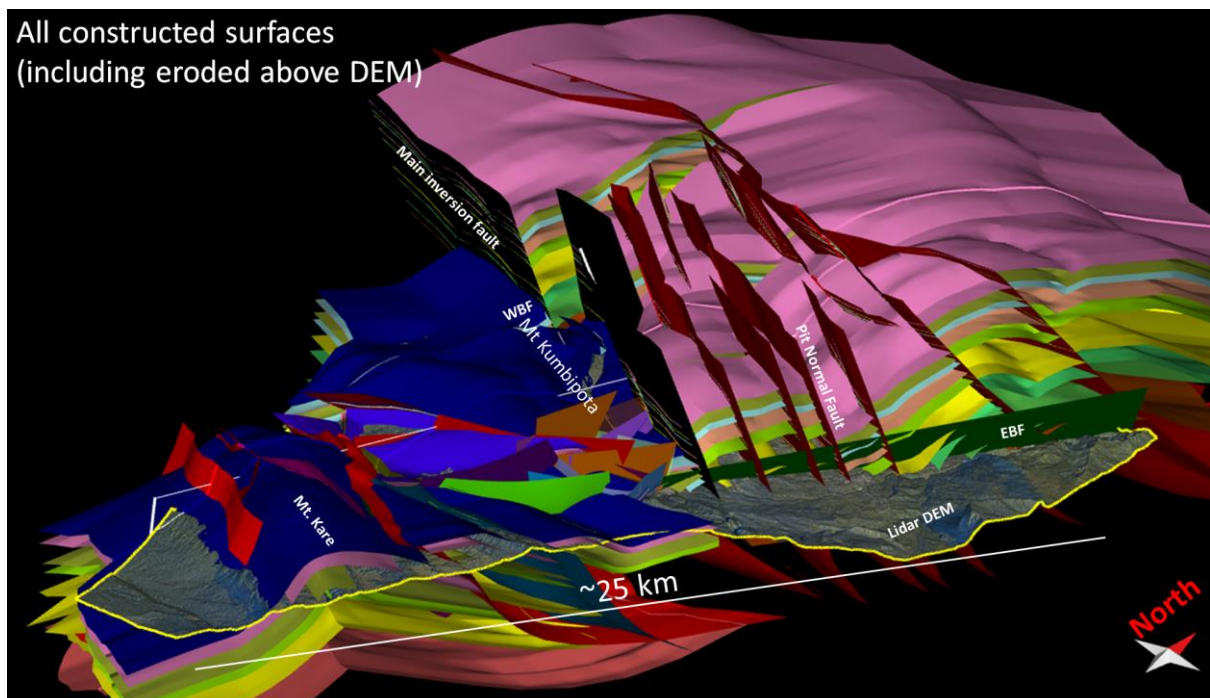


Figure 12. The 3D model constructed from ~100 cross-sections that were made using the LIDAR data. The LIDAR DEM is shown as well as surfaces below and those eroded-off above the ground. Faults are red except the EBF which is green and brown. Horizons are coloured according to lithology. EBF=Eastern Boundary Fault; WBF=Western Boundary Fault.

Discussion

Corbett (1994) suggested that many of the copper-gold deposits in Papua New Guinea were controlled by movements across underlying NNE-trending lineaments in the basement which caused local dilation. He applied this to the Porgera deposit along the Porgera Transfer Zone as shown in Figure 3. Hill et al (2002) and Gow et al (2002) expanded on this notion and Hill (2004) developed a conceptual 3D model for the tectonic evolution (Figure 5). This study has demonstrated the presence of the Porgera Transfer Zone as a significant crustal lineament across the country that was probably reactivated during Mesozoic and Tertiary tectonic events, including rifting, breakup and orogenesis. The progressive thrusting of the PNG margin from 12 Ma to the present shown in Figure 4 illustrates that the Porgera intrusive was emplaced during the peak of compressional orogenesis and that the feed pipe was probably subsequently dismembered by further low-angle thrusts. The new regional LIDAR data has proven instrumental in mapping the area and constructing a semi-regional 3D model, but also in testing the hypothesis of dilation. It is clear from the images that there are significant zones of extension in pull-apart basins and graben associated with dextral offset across the Porgera Transfer Zone (Figures 8, 9 and 10). If the extensional zones are found to coincide with significant magnetic and gravity anomalies there is potential for new sub-surface copper-gold discoveries.

Acknowledgments: We would like to thank the Porgera Joint Venture for commissioning and facilitating this work and for allowing publication. We also thank Petex for ongoing access to the Move™ software at the University of Melbourne for A/Prof. Sandra McLaren.

References

- Corbett G. J. 1994. Regional structural control of selected Cu/Au occurrences in Papua New Guinea. *In: Rogerson L. ed. Proceedings of the Papua New Guinea Geology, Mining and Exploration Conference 1994*, pp. 57–70. Australasian Institute of Mining and Metallurgy, Melbourne.
- Crowhurst P.V., Hill K.C., Foster D.A. & Bennett A.P., 1996. Thermochronological and Geochemical Constraints on the Tectonic Evolution of Northern Papua New Guinea. *In: Hall R. (ed) Tectonic Evolution of SE Asia*. Geological Society of London Special Publication No. 106, 525-537.
- Davies H. L. 1983. *Department of Minerals and Energy 1:250 000 geological map and explanatory notes, Sheet SB/54-8, Wabag*. Geological Survey of Papua New Guinea, Port Moresby.
- Davies H. L. 1991. Regional geologic setting of some mineral deposits of the New Guinea region. *In: Rogerson R. ed. Proceedings of the Papua New Guinea Geology, Exploration and Mining Conference, 1991, Rabaul*, pp. 49–57. Australasian Institute of Mining and Metallurgy, Melbourne.
- Gow P. A., Upton P., Zhao C. & Hill K. C. 2002. Copper-gold mineralisation in New Guinea: numerical modelling of collision, fluid flow and intrusion-related hydrothermal systems. *Australian Journal of Earth Sciences* 49, 753–771.
- Gunson M. J. 2000. Stratigraphic reconstruction of the Porgera Region, Enga Province, Papuan Fold and Thrust Belt, Papua New Guinea. PhD thesis, (unpublished) University of Western Australia. 203 pages.
- Gunson M. J., Hall G. & Johnston M. 2000. Foraminiferal colouration index as a guide to hydrothermal gradients around the Porgera Intrusive Complex, Papua New Guinea. *Economic Geology* 95, 271–282.
- Gunson, M.J., Haig, D.W., Kruman, B., Mason, R.A., Perembo, R.C.B., and Stewart, R., 1997, Stratigraphic reconstruction of the Porgera region, Papua New Guinea: Australasian Institute of Mining and Metallurgy, PNG [Papua New Guinea] Geology, Exploration, and Mining Conference, Madang, October 1997, p. 99–108.
- Hill K.C. & Hall R. 2003. Mesozoic-Tertiary Evolution of Australia's New Guinea Margin in a West Pacific Context. *In: Hillis R.R. & Muller R.D. (eds) Evolution and Dynamics of the Australian Plate*. pp. 265-290. Geological Society of Australia Special Publication 22 and Geological Society of America Special paper 372.
- Hill K.C. 2004. 2D and 3D structure of the Porgera-Mount Kare Transfer Zone, PNG. 3D-Geo report and powerpoint to the Porgera JV, October 2004 (unpublished).
- Hill K.C., Kendrick R.D., Crowhurst P.V. & Gow P., 2002. Predicting Cu-Au mineralisation in New Guinea: 1. Tectonics, lineaments, thermochronology and structure. *Australian Journal of Earth Sciences* 49, 737-752.
- Hill K.C., Mahoney L. & McLaren S., 2020. Compressional evolution of the PNG margin; a tale of two collisions. *AAPG Search and Discovery Article #30661* (2020). 40 pages. http://www.searchanddiscovery.com/documents/2020/30661hill/ndx_hill.pdf

-
- Mahoney L., McLaren S., Hill K., Kohn B., Gallagher K & Norvick M. 2019. Late Cretaceous to Oligocene burial and collision in western Papua New Guinea: Indications from low-temperature thermochronology and thermal modelling. *Tectonophysics* 752, p. 81-112.
- Nash C. and Associates Pty Ltd 2011. Interpretation of stereoscopic aerial photographs and satellite imagery, Porgera area, Papua New Guinea. Report for Barrick (Australia Pacific Ltd) (unpublished). 43 pages.
- Richards J. P. & McDougall I. 1990. Geochronology of the Porgera gold deposit, Papua New Guinea. resolving the effects of excess argon on K–Ar and $^{40}\text{Ar}/^{39}\text{Ar}$ age estimates for magmatism and mineralisation. *Geochimica et Cosmochimica Acta* 54, 1397–1415.
- Thornton R. C. N., Emmett J. K., Laslo J. A. & Gottschalk R. R. 1996. Integrated structural and stratigraphic analysis in PPL 175, Papuan Fold Belt, Papua New Guinea. In: Buchanan P. G. ed. *Petroleum Exploration, Development and Production in Papua New Guinea, Proceedings of the 3rd Papua New Guinea Petroleum Convention, Port Moresby*, pp. 195–215. Papua New Guinea Chamber of Mines, Port Moresby.
- Zahirovic, S., Seton, M., Müller, R., 2014. The Cretaceous and Cenozoic tectonic evolution of Southeast Asia. *Solid Earth (EGU)* 5, 227–273.